Contents lists available at ScienceDirect

Renewable Energy

journal homepage: www.elsevier.com/locate/renene

Photovoltaic power resource at the Atacama Desert under climate change

S. Bayo-Besteiro *, L. de la Torre, X. Costoya, M. Gómez-Gesteira, A. Pérez-Alarcón, M. deCastro, J.A. Añel *

EPhysLab, CIM-UVigo, Universidade de Vigo, Ourense, Spain

ARTICLE INFO

Keywords:
Photovoltaic power under climate change
Atacama
Irradiance
Temperature
Climate models
Climate scenarios

ABSTRACT

The Atacama desert is a region with exceptional conditions for solar power production. However, despite its relevance, the impact of climate change on this resource in this region has barely been studied. Here, we use regional climate models to explore how climate change will affect the photovoltaic solar power resource per square meter (PV_{res}) in Atacama.

Models project average reductions in PV_{res} of 1.5% and 1.7% under an RCP8.5 scenario, respectively, for 2021-2040 and 2041-2060. Under RCP2.6 and the same periods, reductions range between 1.2% and 0.5%. Also, we study the contribution to future changes in PV_{res} of the downwelling shortwave radiation, air temperature and wind velocity. We find that the contribution from changes in wind velocity is negligible. Future changes of downwelling shortwave radiation, under the RCP8.5 scenario, cause up to 87% of the decrease of PV_{res} for 2021-2040 and 84% for 2041-2060. Rising temperatures due to climate change are responsible for drops in PV_{res} ranging between 13%–19% under RCP2.6 and 14%–16% under RCP8.5.

We conclude that climate change has the potential to impact the PV_{res} in the Atacama region while retaining exceptional conditions for solar power production.

1. Introduction

According to the Paris Agreement, urgent action is needed to limit global warming to 1.5 °C [1]. Notwithstanding, in 2021 global CO_2 emissions from the burning of fossil fuels and industrial processes increased to reach their highest annual level with 36.3 Gt/year [2]. On the other hand, renewable energies have seen an increase in installed capacity by 110% during the last ten years in a path to reduce emissions, being wind and solar power the ones with a more significant boost. Worldwide, between 2012 and 2021, total solar photovoltaic power installed capacity increased by 819% (746,641 MW) [3], and by 2050 is expected to grow 996% (7,772 GW) and to rise 8,519 GW [4].

In Chile, the total solar power installed capacity has increased by 456% (3,892 MW) in the period 2015–2021, and currently, solar energy represents 25% (4,468 MW) of the total renewable installed capacity. Of this, photovoltaic power (PV) represents 97% of the total solar power capacity installed (4,360 MW) [5], and it is expected to cover 30% of the energy supply in Chile in 2030 [6]. In the north-central part of the country is located the Atacama Desert. With an area of 105,000 km^2, it covers most of the Antofagasta region and the northern part of the Atacama region [7]. It is one of the driest places in the world and one of the few where annual irradiance exceeds 2,500 kWh/m^2 [8]. On account of these characteristics, Atacama has exceptional conditions for producing solar power, and effectively, the solar power installed capacity in this region represents 92.9% of the total installed capacity in Chile (4,150 MW) [9]. The potential of Atacama for solar energy production has made it called "the solar El Dorado" [10].

Therefore, the rapid growth of solar power over the last few years in this region, coupled with its future development in the country [11], calls for complete knowledge of the changes induced by climate change in the region and their impacts, which can pose challenges for the generation of solar power and energy security [12]. This is important both from the point of view of country-level planning and for climate services [13]. Also, better information can provide benefits in the form of improved exploitation of the solar resource. However, such an assessment with a regional focus and studying the different climatic variables that affect it has not been performed to date. This is despite the fact that in the scientific literature there are many studies on solar energy production focused on this region. Some have analysed the solar spectrum in the Atacama Desert [14,15], which is essential for the development of solar technologies, and others searched the locations with the greatest potential for solar energy and the least impact on the environment [16,17]. Some studies for the region have

* Corresponding authors.
E-mail addresses: s.bayo@uvigo.es (S. Bayo-Besteiro), ltr@uvigo.gal (L. de la Torre), xurxocostoya@uvigo.es (X. Costoya), mggesteira@uvigo.es (M. Gómez-Gesteira), albenis.perez.alarcon@uvigo.es (A. Pérez-Alarcón), mdecastro@uvigo.es (M. deCastro), j.anhel@uvigo.gal (J.A. Añel).

https://doi.org/10.1016/j.renene.2023.118999
Received 14 October 2022; Received in revised form 5 June 2023; Accepted 5 July 2023

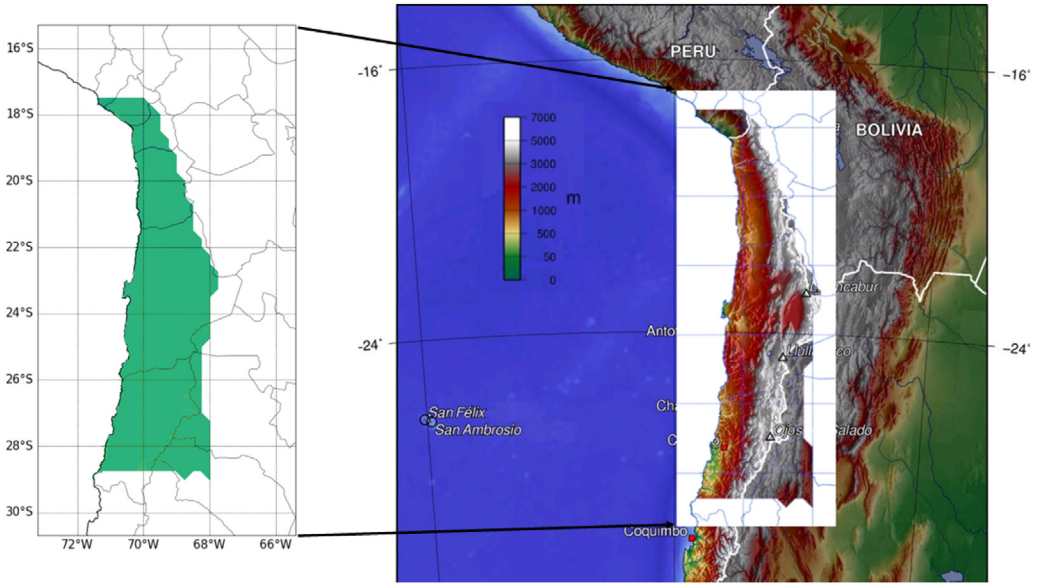

Fig. 1. Area of study. The Atacama Desert.

focused on the use of hybrid models which combine concentrated solar power and photovoltaic systems with thermal energy storage [18–20]. Secondary applications and impacts have also been researched, such as technologies to produce solar hydrogen [21,22] or analyze the soil composition to define cleaning strategies for solar panels [23]. Other works have analysed the impact of climate change on meteorological variables that are someway related to PV production. They have concluded that for different periods of the 21st century, the length of heat waves, the number of extremely warm days, and the intensity of storms will increase, and annual precipitation will decrease [24,25]. The few works providing information on the impacts of climate change on solar power are not specific for the region, and they show that, by the end of this century, PV output is expected to be between 2% and 4% less than compared to 1980-1999 [26] and that changes in the surface-downwelling shortwave radiation (RSDS, 0.2-0.4 μm) are the main cause of the variability in solar power in the Atacama Desert [27]. Other works focused on this region only analysed irradiance [14,15].

However, photovoltaic energy generation relies on not only RSDS [28], but also other variables, such as surface air temperature (TAS) and surface wind velocity (sfcWind). In this vein, the existing literature is insufficient to provide useful meteorological and climatological information for PV generation in the Atacama region. For example, TAS affects the panel efficiency and sfcWind causes variations in the temperature of the solar panels [29]. Knowing how these variables will be affected by climate change in the future and how they combine with RSDS is essential to avoid efficiency losses in energy generation [30,31]. Moreover, the exposition to very high temperatures could cause an increase in the degradation of PV panels [32]. Therefore, knowing better the changes in these variables helps to implement adaptation actions to reduce the impact of climate change on solar power generation and determine the profitability of future plants in the region of study.

Hence, this work aims to analyse the impact of climate change on the main variables for PV generation (RSDS, TAS, and sfcWind) for the region of the Atacama Desert and how they drive changes in PV power generation. To do this, we use a set of regional climate models (RCMs) and theory on PV production [33]. Factors such as the impact of aerosols and dust that could deposit on solar panels are not evaluated, as they are not resolved by climate change models, are beyond the scope of this work, and need other types of analysis [34].

The remainder of the paper is organised as follows: First, we describe the data we used and the methodology, including the computation of solar power production; Next, we present our results showing the future model projections of the main variables, and then, we apply theory to compute the changes on solar power production. Last, we analyse the results and present the conclusions.

2. Data and methodology

2.1. Region of study

The region of study is the Atacama Desert (see Fig. 1), an arid region in northern Chile that is 1,000 to 1,100 km long from north to south. The Atacama Desert is on the west slope of the central Andes between 15 °S and 30 °S at elevations between sea level and 3500 m above sea level [35]. The coast range covers around 1,500 m in elevation, with individual peaks reaching 2,000 m. In the interior, a raised depression extends north and south and forms the high Tamarugal Plain at an elevation of more than 900 m. Along the northeastern extends the Atacama Plateau, which reaches 4,000 m [7].

2.2. Data

TAS, RSDS and 10-m u (the zonal component of velocity) and v (the meridional component of velocity) components of sfcWind were obtained from the Coordinated Regional Climate Downscaling Experiment (CORDEX) simulations, the program sponsored by the World Climate Research Program (WCRP) to develop an improved framework for generating regional-scale climate projections for impact assessment and adaptation studies worldwide [36]. The CORDEX simulations are selected with the highest possible spatial resolution (0.22° x 0.22°) for the South America region (SAM) under the RCP8.5 and RCP2.6 scenarios. The RCP8.5 is a Representative Concentration Pathway (RCP) that consists in a greenhouse gas concentration trajectory that delivers global warming at an average of 8.5 W/m^2 across the planet, and RCP2.6 refers to 2.6 W/m^2 [37]. We selected RCP2.6 and RCP8.5 scenarios because, for the variables analysed in this work, they are the only available in the CORDEX SAM region with the necessary spatial resolution.

Data from simulations was retrieved from CORDEX repositories as monthly mean files [38] and used to analyse the PV variability both for the near (2021–2040) and mid-term (2041–2060) future periods. These future periods are the most relevant for stakeholders (as per consultation with energy sector developers in the region) in the renewable energy sector. Historical simulations (1980–2015) were also

Table 1
GCMs (Global Climate Models) forcing REMO2015 and label used here to refer to the different coupled models [39].

Label	GCM	RCM
M1	MOCH- HadGEM2-ES [40]	
M2	MPI-M-MPI-ESM-LR [41]	REMO2015[39]
M3	NCC-NorESM1-M [42]	

considered for comparison purposes. Only three RCMs from CORDEX met the conditions of data availability (scenarios, region and horizontal resolution) requested (see Table 1).

HadGEM2 is a model developed by the Met Office Hadley Centre. The model includes the components of the carbon cycle, but it excludes the nitrogen cycle. HadGEM2 is a stable model which represents a realistic state of the climate, vegetation, and ocean biology. As a shortcoming, it presents some areas where there is a large over-prediction of dust emissions [40]. MPI-ESM is developed by the Max Planck Institute for Meteorology. It is a coupled climate model that includes dynamic vegetation and an interactive carbon cycle. The model response to increasing concentrations of atmospheric CO_2 is within the mid-range of estimates of other comprehensive GCMs and is amplified by cloud processes. Aerosol radiative interactions play a relatively minor role [41]. NorESM1 is based on the Community Climate System Model version 4 (CCSM4) operated at the USA National Center for Atmospheric Research. As issues to consider for this study, NorESM1 underestimates cloudiness and, over the continents, the global mean near-surface air temperatures [42]. Regarding REMO, it does not present issues relevant to this work; also, it has been proved that it is able to simulate the mean annual climatic features in all domains quite reasonably [43]. These three RCMs have already been used in previous climatic analyses to research extreme precipitation and temperatures in the region studied here [44–46].

To evaluate the reliability of the CORDEX simulations, we compared them to the ERA5 reanalysis [47]. ERA5 is the fifth-generation atmospheric reanalysis produced by the European Centre for Medium-Range Weather Forecasts (ECMWF), covering the period from January 1950 to the present and many studies have evaluated its performance [48–56]. Its spatial resolution consists of a 30 km grid. The ERA5 variables used to evaluate the outputs from CORDEX models were surface solar radiation downwards, 2 m temperature, and 10 m u and v wind components.

2.3. Methodology

2.3.1. Skill of CORDEX simulations

To select the CORDEX model that best reproduces the historical TAS, RSDS, and 10 m sfcWind components, we computed the normalised root mean square error ($RMSE_N$) (see relation 1) for each variable and model [33]. Fig. 2 shows the results in percentage.

$$RMSE_N = \frac{RMSE}{\langle x \rangle} \cdot 100 \tag{1}$$

2.3.2. Solar photovoltaic resource calculation

The solar photovoltaic power resource (PV_{res}) represents the value of solar energy available, taking into account the RSDS and the variations in the efficiency of the photovoltaic cell caused by changes in temperature.

PV_{res} is calculated from RSDS (see Eq. (2)) [33] and takes into account the correction related to the efficiency of PV solar cells, which decreases as their temperature increases [57].

$$PV_{res} = PV_{pot} \cdot RSDS_{STC} = P_R \cdot RSDS \tag{2}$$

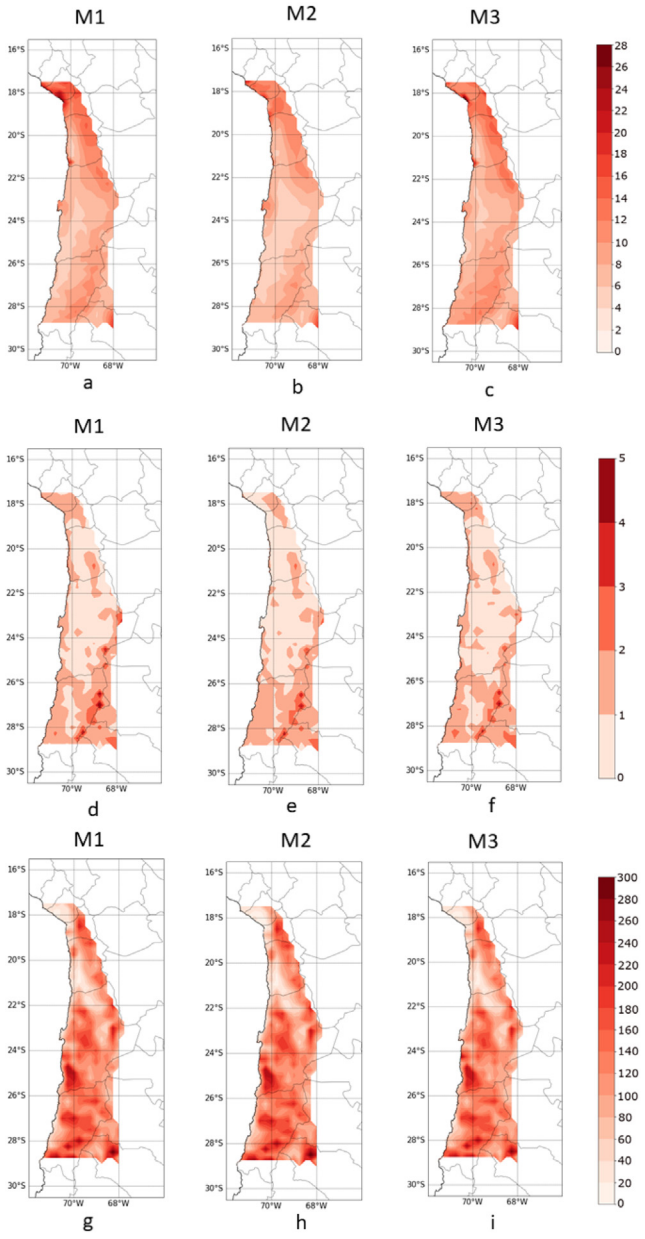

Fig. 2. RMSE (%) calculated for RSDS (a,b,c), TAS (d,e,f) and scfWind (g,h,i) comparing ERA5 to CORDEX simulations. M1, M2 and M3 are the CORDEX models (see Eq. (1)).

Where PV_{pot} is the power generation potential, $RSDS_{STC}$ = 1,000 W m^{-2} is the RSDS in standard test conditions, and P_R is the performance ratio formulated to account for the influence of temperature into the PV cells efficiency, according to the following relation:

$$P_R = 1 + \gamma[T_{cell}(t) - T_{STC}] \tag{3}$$

where T_{STC} = 25 °C is the temperature in standard test conditions and γ = −0.005 $°C^{-1}$ is the efficiency temperature coefficient given in the literature [58]. T_{cell} is the temperature of the PV cell calculated considering the effects of TAS, RSDS and scfWind (Eq. (4)) [58,59].

$$T_{cell} = c_1 + c_2 TAS(t) + c_3 RSDS(t) + c_4 scfWind(t) \tag{4}$$

with c_1 = 4.3 °C, c_2 = 0.943, c_3=0.028 °C m^2 W^{-1} and c_4 = −1.528 °C sm^{-1}

Grouping the relations (2), (3) and (4) the expression of PV_{pot} becomes:

$$PVpot = \alpha_1 RSDS + \alpha_2 RSDS^2 + \alpha_3 RSDS \cdot TAS + \alpha_4 RSDS \cdot scfWind$$
$$\alpha_1 = 1.1035 \cdot 10^{-3}, \alpha_2 = -1.4 \cdot 10^{-7}, \alpha_3 = -4.715 \cdot 10^{-6}, \alpha_4 = 7.64 \cdot 10^{-6} \quad (5)$$

The values of α_1, α_2, α_3 *and* α_4 have been established in the literature [58].

PV_{res} is averaged annually for each grid point for each model using a common grid with the same spatial resolution (0.22° × 0.22°). Then, the multi-model mean is computed.

Also, we analysed how the changes in TAS and scfWind induced changes in PV power generation. To do it we computed ΔPV_{res} (see Eq. (6)).

$$\Delta PV_{res} = \Delta PVpot \cdot RSDS_{STC} \quad (6)$$

$$Being \Delta PVpot : \Delta PVpot$$
$$= \Delta RSDS(\alpha_1 + \alpha_2 RSDS + 2\alpha_2 RSDS + \alpha_3 TAS + \alpha_4 VWS) +$$
$$\alpha_3 RSDS \cdot \Delta TAS + \alpha_4 RSDS \cdot \Delta VWS$$
$$+ \alpha_3 \Delta RSDS \cdot \Delta TAS + \alpha_4 \Delta RSDS \cdot \Delta VWS \quad (7)$$

With this relation, we can attribute changes in PV_{res} to changes in TAS, taking ΔRSDS = 0 and ΔVWS = 0. In the same way, taking ΔTAS = 0 and ΔRSDS = 0 enables us to attribute changes in PV_{res} to changes in scfWind.

To obtain the data results and the plots, we used a Python code [60]. This code is included as supplementary electronic material and is available via Zenodo [61] to comply with scientific reproducibility [62].

3. Results and discussion

3.1. Capability of CORDEX simulations to reproduce RSDS, TAS and sfcWind

Fig. 2 shows the results of the RMSE for the different variables from CORDEX simulations involved in PV production. The RMSE for RSDS shows variations between 1%–10% for almost the entire region of study, with the highest values in the mountainous areas and the minimum in the centre of the region and near the coast. TAS shows variations between 1%–5%, finding the highest values in the south and the minimum in the north and centre. That said, for most of the regions, variations are not higher than 3%. For scfWind, RMSE ranges between 30%–200%, being, in fact, greater than 100% for most of the region.

The values of RMSE for scfWind showed the poor capability of CORDEX simulations to reproduce this variable. We guess that it can be due to the complex orography of the region studied, a strip of land between sea and mountains. Other studies found locations with complex orography where the CORDEX models were not able to accurately represent the wind due to its limited resolution [63,64].

Issues with scfWind are negligible in this case, as the impact of this variable on PV_{res} is less than 1%.

3.2. Historical mean values

The results of the mean PV_{res} calculated with CORDEX simulations for the historical period (1980–2015) show values between 190 W/m^2 and 336 W/m^2, with almost the entire region above 280 W/m^2, and the higher values in the mountainous areas of the south-east (see Fig. 3). The mean values of RSDS show values between 191 W/m^2 and 303 W/m^2. The lowest values of RSDS are in the north and in the south east of the region (see supplementary material). The results of the mean values for the same period for TAS show values between −15 °C and 23 °C, with the lowest values of TAS in the mountainous areas of the east and the highest in the centre and coastal areas. scfWind shows values between 1 m/s and 9 m/s, with the highest in the south east (see supplementary material).

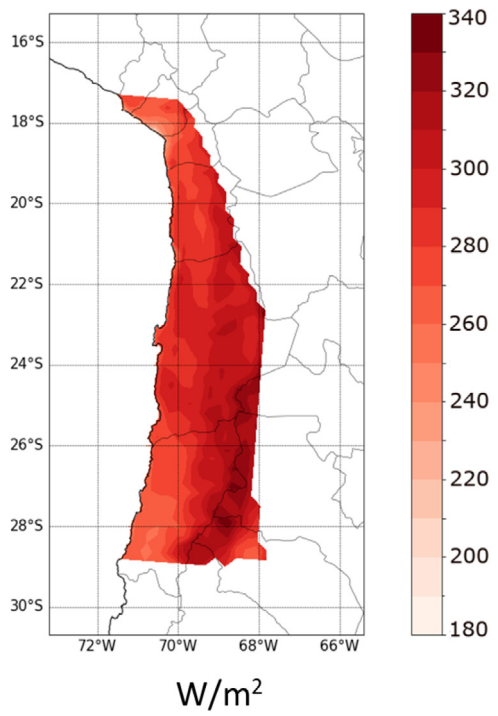

Fig. 3. Values of PV_{res} (W/m^2) for the historical period (1980–2015). The image shows a multimodel mean (M1, M2 and M3).

In order to assess the accuracy of the models when representing PV_{res}, we calculated the root square mean error (RSME) for it (by comparing the CORDEX simulations to ERA5 data), finding that the maximum PV_{res} RSME values are less than 1% for the whole region (see supplementary material).

3.3. Projected changes in RSDS and TAS

Future changes in RSDS and TAS are evaluated for the near future (2021–2040) and the mid-term (2041–2060) with respect to the historical period (1980–2015) for RCP2.6 and RCP8.5 scenarios. RSDS (see Fig. 4), in the west area of the Atacama Desert, shows decreases for both periods and both scenarios, more accentuated for the mid-term future for the RCP8.5, with a reduction of 7.5 W/m^2 for the south and north of the Atacama Desert. For the RCP2.6, the west area of the Atacama desert shows decreases between 4 W/m^2 and 6 W/m^2. In the east area, RSDS shows an increase, especially for the near future in both, that could reach 5 W/m^2 for the RCP8.5 and 2.6 W/m^2 for RCP2.6. The central area, for 2041–2060, shows a decrease between 1 W/m^2 and 4 W/m^2 for RCP8.5 and between 0.5 W/m^2 and 2 W/m^2 for the RCP2.6.

The projections of TAS show an increase in its values, especially in the southeast. For RCP2.6, for the near future, the temperature shows an increase greater than for the mid-term future that could reach 1.2 ℃ and 1 ℃, respectively.

The results for the RCP8.5 for the mid-term future show an increase in temperature that could reach 4.5 ℃. For the near future, the projections in TAS show an increase between 0.5 ℃ and 2.5 ℃ (see Fig. 5).

3.4. Changes in PV_{res}

Given the complex orography of the region studied, surrounded by the coast, and being a plateau at high altitude, the output from the

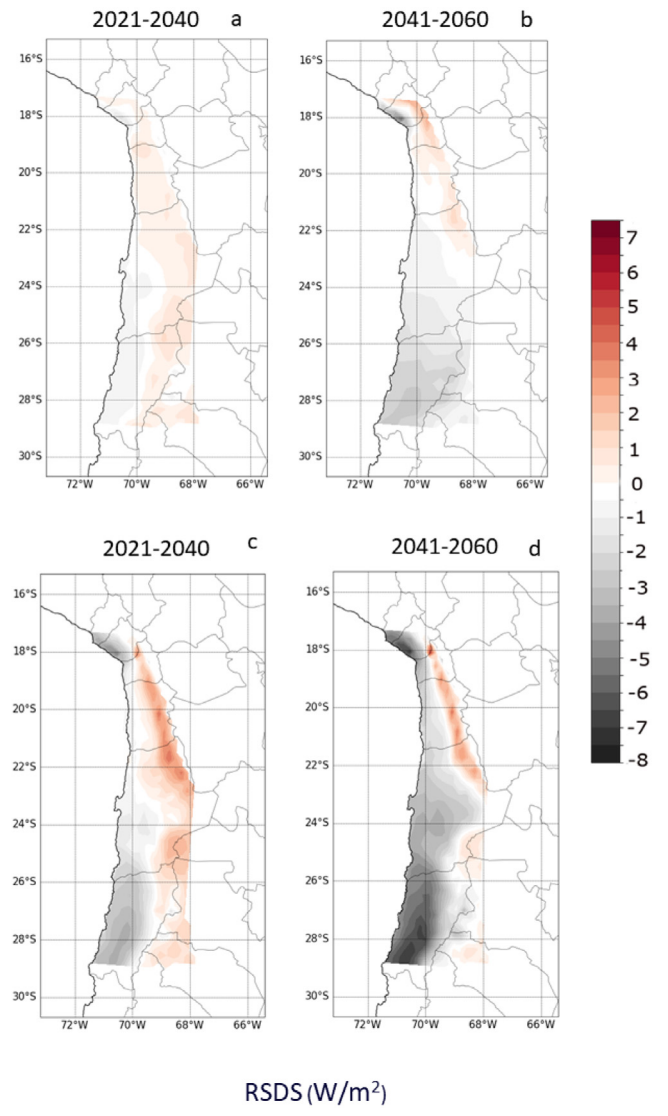

Fig. 4. Changes projected (multimodel mean) regarding the historical period (1980–2015), for RSDS for the RCP2.6 (a,b) and the RCP8.5 (c,d). The left panels correspond to 2021–2040, and the right ones to 2041–2060.

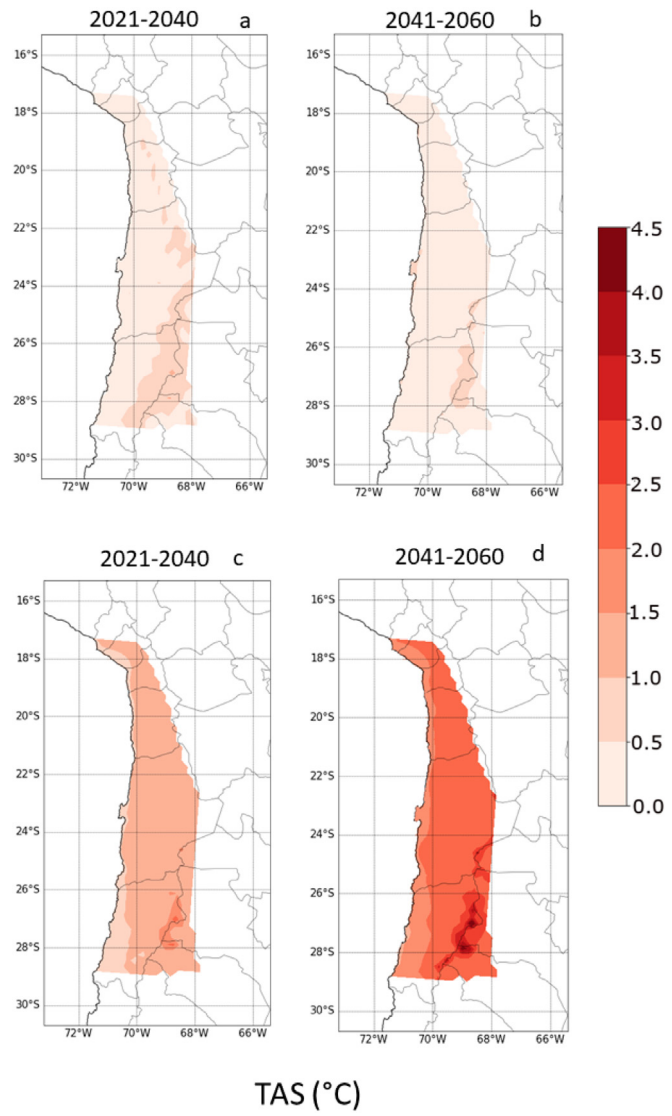

Fig. 5. Changes projected for TAS, for RCP2.6 (a,b) and for RCP8.5(c,d) compared to 1980–2015. The image shows the multimodel mean.

models is prone to show singularities, for example, when the model grid takes a small part of land that could be considered as sea. This results in outliers in the data from the simulations. To avoid their impact on the interpretation of the results of PV_{res}, we considered only those values that lie in the 2σ interval, being σ, the standard deviation. Here $\sigma = 4.27$ W/m^2.

For the RCP2.6 scenario, the results of the PV_{res} projections show a slight increase in the northeast of the region with changes between 0.5% and 1% and a decrease in the south of the Atacama desert for the mid-term future. For the near future, the average reduction for the region is 1.23%, and for the mid-term future is 0.52% (see Fig. 6(a,b)).

The PV_{res} projections for the RCP8.5 show a reduction for the two periods analysed in this work. For the near future, the average reduction for the region is 1.53%; meanwhile, for the mid-term future, we found a decrease up to 4% in the south of the region, and the average value is 1.72% (see Fig. 6(c,d)).

Splitting the analysis by contributing factors, for RCP2.6, the contribution of changes in TAS to change of ΔPV_{res} shows values between 0%–30% over most of the area of study for the two periods analysed (see Fig. 7 (a,b)) with average values for all the region of 12.91% for the near future and 19.52% for the mid-term (see Table 2 for the average values). In the figure, some points reach values near 90%; however, they should be interpreted with caution, as they are near the mountain areas, which are prone to outliers. For the RCP8.5, the changes in PV_{res} due to TAS changes range between 0% and 30% over most of the area for the two periods analysed (see Fig. 7 (c,d)), with average values of 13.62% for the near future and 15.75% for the mid-term (Table 2). We note that the values shown here are positive because they are the percentual part of changes in PV_{res} due to changes in TAS.

The contribution of changes in scfWind to the changes of ΔPV_{res} for the RCP2.6 and RCP8.5 scenarios show values of PV_{res} between −3.3% and 3.3% for the near future. For the mid-term future, this contribution ranges between −3.48% and 3.37% (see Fig. 8). For the RCP2.6 scenario, the average contribution is 0.3% for the near future and −0.27% for the mid-term. For RCP8.5, the values are −0.34% for the near future and 0.16% for the mid-term (see Table 2).

The contribution of change in RSDS to the changes of ΔPV_{res} that this variable is responsible for, will be the remaining part that is not attributable to the other two (TAs and sfcWind). Therefore, taking the mean values for the whole region of study, for the RCP2.6, the decrease of RSDS is responsible for 87% and 81% of the total reduction of PV_{res} for 2021–2040 and 2041–2060, respectively. For the RCP8.5, the

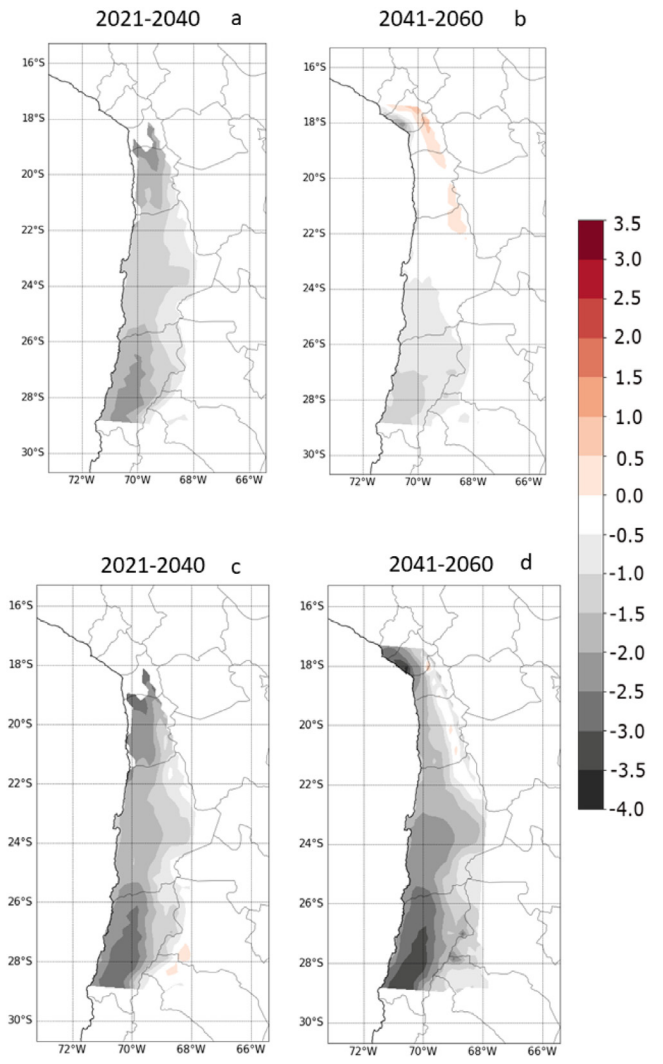

Fig. 6. ΔPV_{res} (%) for the near future (a,c) and mid-term future (b,d) under the RCP2.6 (a,b) and RCP8.5 (c,d) compared to 1980–2015. The image shows the multimodel mean.

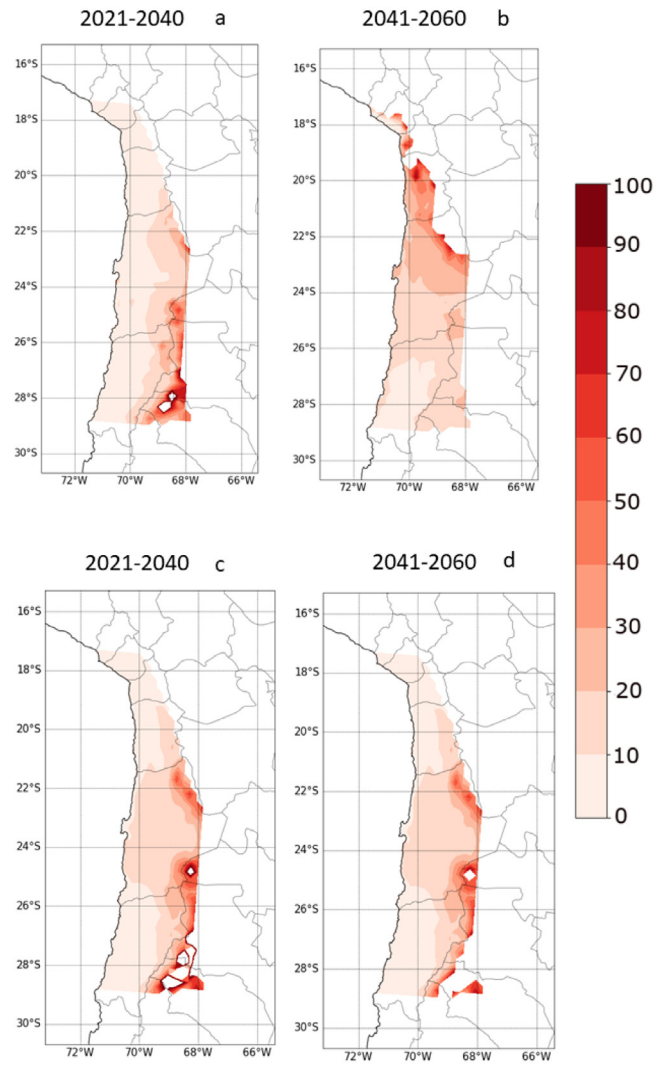

Fig. 7. Contribution of change in TAS to the changes of ΔPV_{res} (%) for the near future (a,c) and mid-term future (b,d) under the RCP2.6 (a,b) and RCP8.5 (c,d) compared to 1980–2015. The plot shows the multimodel mean. Given the complex orography in high mountain areas, the model shows outliers. Because of it, in the plots, the results for some points of mountainous areas are not shown.

Table 2
ΔPV_{res}(%) and the contribution of changes(%) in TAS, scfWind and RSDS to the changes of ΔPV_{res} for RCP2.6 and RCP8.5 scenarios and for the near future and mid-term periods.

	RCP2.6		RCP8.5	
	(2021–2040)	(2041–2060)	(2021–2040)	(2041–2060)
ΔPV_{res} (%)	1.23	0.52	1.53	1.72
Contribution of changes in TAS to ΔPV_{res}(%)	12.91	19.52	13.62	15.75
Contribution of changes in scfWind to ΔPV_{res} (%)	0.3	−0.27	−0.34	0.16
Contribution of changes in RSDS to ΔPV_{res}(%)	86.79	81	86.72	84.08

decrease of RSDS is responsible for 87% and 84% of the total reduction of PV_{res} for 2021–2040 and 2041–2060, respectively (Table 2).

Unfortunately, the lack of scientific literature on the study of solar photovoltaic power generation and the variables which caused its variability for the region of study on an annual scale precludes the comparison of these results.

In order to present the results in an integrated way, we show the uncertainty by means of showing the standard deviation of the model's mean PV_{res}. To do this, we calculate the annual mean PV_{res} for each model for the whole area of study, and then we calculate the multimodel mean. Then, we compute the corresponding standard deviation. The black line represents the annual mean, and the shadow area is the interval of the standard deviation 9. The results show that the standard deviation (σ) values range between ±5 W/m^2 and ±8 W/m^2.

For future works, other variables impacting the power generation of solar panels could be taken into account. For example, previous studies have shown that soiling of solar panels decreases power generation in the Atacama desert [65,66]; however, differences in decreases are big depending on the region, ranging from almost negligible in the highest altitudes and southern part of the desert, where we find the largest changes in PV_{res} due to the wind, to up to 39% in the northern coastal part [67]. In this way, it can be speculated if future changes in wind regimes could change the distribution of aerosol loads.

Also, an improvement to this work would need an advancement in the capability of models to reproduce the representation of winds in

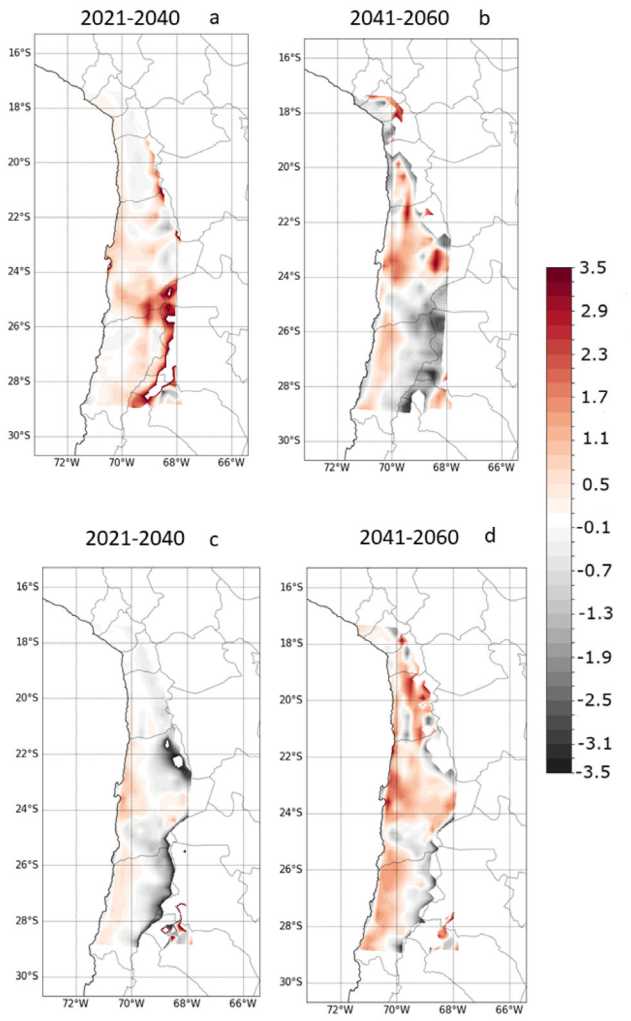

Fig. 8. Contribution of change in scfWind to the changes of ΔPV_{res} (%) for the near future (a,c) and mid-term future (b,d) under the RCP2.6 (a,b) and RCP8.5 (c,d) compared to 1980–2015. The plot shows the multimodel mean. Given the complex orography in high mountain areas, the model shows outliers. Because of it, in the plots, the results for some points of mountainous areas are not shown.

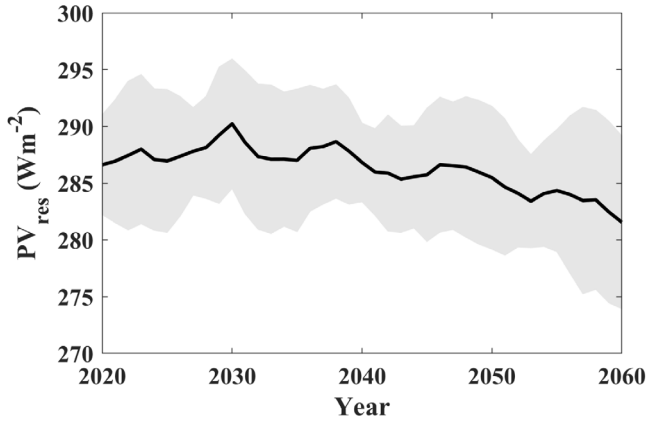

Fig. 9. Annual value of PV_{res} obtained with the models from Eq. (1). The black line is the mean annual value of the three models, and the shadow area shows the standard deviation around the mean (σ).

mountainous regions. Furthermore, we could only use three CORDEX models for these variables and this region. These issues reveal that increasing the data and studies for the region studied is urgent, mainly because of its relevance for energy production.

4. Conclusions

This study analysed future variations in the solar photovoltaic power resource in the Atacama Desert during the period 2021–2060 by means of an ensemble of three RCMs from the CORDEX project for two pathway emissions scenarios, RCP2.6 and RCP8.5. The accuracy of these simulations was validated by comparing simulated RSDS, TAS and sfcWinds with the values obtained from ERA5 for 1980–2015. Our main findings can be summarised as follows:

- RSDS and TAS data from CORDEX are in good agreement with those from ERA5; however, we conclude that the models are not able to represent the values of scfWind correctly.
- A decrease in RSDS in the west and central area of the Atacama Desert was observed in both 2021–2040 and 2041–2060 for the two scenarios analysed, especially for the mid-term in the RCP8.5. In the east area, RSDS shows an increase, especially for the near future in the RCP8.5. For RCP2.6 and mid-term, the RSDS shows a decrease along all of the Atacama desert except in the east, where an increase is observed.
- The projected changes in TAS show an increase for the two periods and two scenarios and cause a decrease in the projected PV_{res}.
- We obtain an average reduction of 1.23% in PVres under the RCP2.6 for the near future and 0.52% for the mid-term. Under the RCP8.5, the reduction is even higher, with values of 1.53% for the near future and 0.77% for the mid-term.
- The changes in RSDS are the main cause of the variability in PV_{res}: for the RCP2.6 between 87%–81%, and for the RCP8.5 87%–84% (in both for the mid-term and near future, respectively). The increase of TAS is responsible for changes between 13%–19% for the RCP2.6 and 14%–16% for the RCP8.5 (again for the mid-term and near future, respectively). That said, the contribution of the changes in TAS to the reduction in PV_{res} changes depending on the scenario and period. The changes in scfWind caused a negligible impact on PV_{res} in both scenarios.

  Finally, with the goal of more accurate evaluations of the solar resource in this region in the future, it would be desirable to have a more comprehensive set of simulations, with more models with the output variables and spatial resolution necessary available for the region. We recall that from the CORDEX models, only three had the data necessary for our requirements in this study. In this way, with a larger number of models contributing to the multimodel mean, bias in the final results could be smaller. This is something that CORDEX contributors could consider in the future.

CRediT authorship contribution statement

S. Bayo-Besteiro: Conceptualization, Methodology, Investigation, Writing, Data curation. **L. de la Torre:** Methodology, Data curation, Investigation. **X. Costoya:** Data curation, Methodology, Supervision. **M. Gómez-Gesteira:** Supervision, Methodology, Investigation, Validation. **A. Pérez-Alarcón:** Data curation, Software. **M. deCastro:** Supervision, Methodology, Investigation, Validation. **J.A. Añel:** Validation, Conceptualization, Resources, Investigation, Writing, Supervision, Project administration, Funding acquisition.

Declaration of competing interest

The authors declare that they have no known competing financial interests or personal relationships that could have appeared to influence the work reported in this paper.

Acknowledgements

We thank Mikel Illarregi and Magdalena G. Mora from Acciona Energía for their comments and advice on the on-site production of solar photovoltaic energy in the Atacama region. Also, we would to thank Acciona Energía for providing funding during the initial stages of this work, which later led to this paper.

Funding

The EPhysLab is funded by the Xunta de Galicia under the grant ED431C 2021/44 "Programa de Consolidación e Estructuración de Unidades de Investigación Competitivas" (Grupos de Referencia Competitiva). Juan A. Añel is supported by a joint grant of the Ministerio de Universidades and the Universidade de Vigo, under the programme of requalification of Spanish universities. The authors acknowledge the funding for open access from the University of Vigo/Consorcio Interuniversitario do Sistema Universitario de Galicia. X. Costoya is supported by Grant IJC2020-043745-I/MCIN/AEI/ 10.13039/501100011033 by MCIN/AEI/ 10.13039/501100011033 and by the "European Union NextGenerationEU/PRTR".

Appendix A. Supplementary data

Supplementary material related to this article can be found online at https://doi.org/10.1016/j.renene.2023.118999.

References

[1] United Nations, Adoption of the Paris agreement, 21st conference of the parties, Paris, 2015, https://unfccc.int/sites/default/files/english_paris_agreement.pdf. (Accessed 21 July 2021).

[2] International Energy Agency, Global energy review: CO2 emissions in 2021, 2022, https://iea.blob.core.windows.net/assets/c3086240-732b-4f6a-89d7-db01be018f5e/GlobalEnergyReviewCO2Emissionsin2021.pdf.

[3] International Renewable Energy Agency, Renewable capacity statistics 2022, 2022, https://irena.org/-/media/Files/IRENA/Agency/Publication/2022/Apr/IRENA_RE_Capacity_Statistics_2022.pdf. (Accessed 17 August 2022).

[4] International Renewable Energy Agency, Future of solar photovoltaic, 2019, https://www.irena.org/-/media/Files/IRENA/Agency/Publication/2019/Nov/IRENA_Future_of_Solar_PV_2019.pdf.

[5] International Renewable Energy Agency, Renewable capacity statistics 2021, 2021, https://www.irena.org/-/media/Files/IRENA/Agency/Publication/2021/Apr/IRENA_RE_Capacity_Statistics_2021.pdf.

[6] P. Moray, Análisis de largo plazo para el sistema eléctrico nacional de chile considerando fuentes de energía variables e intermitentes informe final, 2018, http://generadoras.cl/media/seminario/180611_Analisis_de_largo_plazo_para_el_sistema_electrico_nacional_de_Chile_considerando_fuentes_de_energia_variables_e_intermitentes.pdf.

[7] Encyclopedia Britannica, Atacama desert, 2019, https://www.britannica.com/place/Atacama-Desert.

[8] J. Ascencio-Vásquez, K. Brecl, M. Topič, Methodology of Köppen-Geiger-Photovoltaic climate classification and implications to worldwide mapping of PV system performance, Sol. Energy 191 (2019) 672–685, http://dx.doi.org/10.1016/j.solener.2019.08.072.

[9] Comisión Nacional de la Energía. Gobiertno de Chile, Energía abierta, 2021, http://datos.energiaabierta.cl/dataviews/245691/capacidad-instalada-de-generacion-sen/. (Accesed 27 December 2021).

[10] L. Dupin, Atacama, the solar Eldorado, Usine Nouvelle (3501) (2017) 44–47, Atacama, l'eldorado solaire, Place: France.

[11] Gobierno de Chile, Energía 2050. política energética de chile, 2022, https://www.energia.gob.cl/sites/default/files/energia_2050_-_politica_energetica_de_chile.pdf. (Accessed 17 August 2022).

[12] J.A. Añel, On the importance of weather and climate change for our present and future energy needs, edited by Troccoli, Dubus and Ellen Haupt, Contemp. Phys. 56 (2) (2015) 206–208, http://dx.doi.org/10.1080/00107514.2015.1006251.

[13] C. Goodess, A. Troccoli, C. Acton, J. Añel, P. Bett, D. Brayshaw, M. De Felice, S. Dorling, L. Dubus, L. Penny, B. Percy, T. Ranchin, C. Thomas, M. Trolliet, L. Wald, Advancing climate services for the European renewable energy sector through capacity building and user engagement, Clim. Serv. 16 (2019) 100139, http://dx.doi.org/10.1016/j.cliser.2019.100139.

[14] A. Marzo, P. Ferrada, F. Beiza, P. Besson, J. Alonso-Montesinos, J. Ballestrín, R. Román, C. Portillo, R. Escobar, E. Fuentealba, Standard or local solar spectrum Implications for solar technologies studies in the Atacama desert, Renew. Energy 127 (2018) 871–882, http://dx.doi.org/10.1016/j.renene.2018.05.039.

[15] A. Marzo, P. Ferrada, F. Beiza, J. Alonso, J. Ballestrín, R. Román, Comparison of atacama desert solar spectra vs. ASTM G173-03 reference spectra for solar energy application, in: International Energy Society. Conference Proceedings, 2016, http://dx.doi.org/10.18086/eurosun.2016.09.01.

[16] A. Suuronen, A. Lensu, M. Kuitunen, R. Andrade-Alvear, N.G. Celis, M. Miranda, M. Perez, J.V.K. Kukkonen, Optimization of photovoltaic solar power plant locations in northern Chile, Environ. Earth Sci. 76 (24) (2017) 824, http://dx.doi.org/10.1007/s12665-017-7170-z.

[17] A. Suuronen, C. Muñoz-Escobar, A. Lensu, M. Kuitunen, N. Guajardo Celis, P. Espinoza Astudillo, M. Ferrú, A. Taucare-Ríos, M. Miranda, J.V.K. Kukkonen, The influence of solar power plants on microclimatic conditions and the Biotic community in Chilean desert environments, Environ. Manag. 60 (4) (2017) 630–642, http://dx.doi.org/10.1007/s00267-017-0906-4.

[18] C. Parrado, A. Girard, F. Simon, E. Fuentealba, 2050 LCOE (Levelized Cost of Energy) projection for a hybrid PV (photovoltaic)-CSP (concentrated solar power) plant in the Atacama Desert, Chile, Energy 94 (2016) 422–430, http://dx.doi.org/10.1016/j.energy.2015.11.015.

[19] R. Bravo, D. Friedrich, Two-stage optimisation of hybrid solar power plants, Sol. Energy 164 (2018) 187–199, http://dx.doi.org/10.1016/j.solener.2018.01.078.

[20] R. Bravo, C. Ortiz, R. Chacartegui, D. Friedrich, Multi-objective optimisation and guidelines for the design of dispatchable hybrid solar power plants with thermochemical energy storage, Appl. Energy 282 (2021) 116257, http://dx.doi.org/10.1016/j.apenergy.2020.116257.

[21] F.I. Gallardo, A. Monforti Ferrario, M. Lamagna, E. Bocci, D. Astiaso Garcia, T.E. Baeza-Jeria, A Techno-Economic Analysis of solar hydrogen production by electrolysis in the north of Chile and the case of exportation from Atacama Desert to Japan, Int. J. Hydrog. Energy 46 (26) (2021) 13709–13728, http://dx.doi.org/10.1016/j.ijhydene.2020.07.050, European Fuel Cell Conference & Exhibition 2019.

[22] J. Armijo, C. Philibert, Flexible production of green hydrogen and ammonia from variable solar and wind energy: Case study of Chile and Argentina, Int. J. Hydrog. Energy 45 (3) (2020) 1541–1558, http://dx.doi.org/10.1016/j.ijhydene.2019.11.028.

[23] P. Ferrada, D. Olivares, V. del Campo, A. Marzo, F. Araya, E. Cabrera, J. Llanos, J. Correa-Puerta, C. Portillo, D. Román Silva, M. Trigo-Gonzalez, J. Alonso-Montesinos, G. López, J. Polo, F.J. Batlles, E. Fuentealba, Physicochemical characterization of soiling from photovoltaic facilities in arid locations in the Atacama Desert, Sol. Energy 187 (2019) 47–56, http://dx.doi.org/10.1016/j.solener.2019.05.034.

[24] S. Feron, R.R. Cordero, A. Damiani, P.J. Llanillo, J. Jorquera, E. Sepulveda, V. Asencio, D. Laroze, F. Labbe, J. Carrasco, G. Torres, Observations and projections of heat waves in South America, Sci. Rep. 9 (1) (2019) 8173, http://dx.doi.org/10.1038/s41598-019-44614-4.

[25] C. Ortega, G. Vargas, M. Rojas, J.A. Rutllant, P. Muñoz, C.B. Lange, S. Pantoja, L. Dezileau, L. Ortlieb, Extreme ENSO-driven torrential rainfalls at the southern edge of the Atacama Desert during the Late Holocene and their projection into the 21th century, Glob. Planet Change 175 (2019) 226–237, http://dx.doi.org/10.1016/j.gloplacha.2019.02.011.

[26] J.A. Crook, L.A. Jones, P.M. Forster, R. Crook, Climate change impacts on future photovoltaic and concentrated solar power energy output, Energy Environ. Sci. 4 (2011) 3101–3109, http://dx.doi.org/10.1039/C1EE01495A.

[27] S. Feron, R.R. Cordero, A. Damiani, R.B. Jackson, Climate change extremes and photovoltaic power output, Nat. Sustain. (2020) http://dx.doi.org/10.1038/s41893-020-00643-w.

[28] R. Hogan, Radiation quantities in the ECMWF model and MARS, 2022, https://www.ecmwf.int/node/18490. (Accessed 17 August 2022).

[29] Seaward, 2021, https://www.seaward.com/gb/support/solar/faqs/00797-how-does-temperature-and-irradiance-affect-i-v-curves/. (Accessed 16 April 2021).

[30] J.K. Kaldellis, M. Kapsali, K.A. Kavadias, Temperature and wind speed impact on the efficiency of PV installations. Experience obtained from outdoor measurements in Greece, Renew. Energy 66 (2014) 612–624, http://dx.doi.org/10.1016/j.renene.2013.12.041.

[31] A. Vasel, F. Iakovidis, The effect of wind direction on the performance of solar PV plants, Energy Convers. Manag. 153 (2017) 455–461, http://dx.doi.org/10.1016/j.enconman.2017.09.077.

[32] V. Poulek, T. Matuška, M. Libra, E. Kachalouski, J. Sedláček, Influence of increased temperature on energy production of roof integrated PV panels, Energy Build. 166 (2018) 418–425, http://dx.doi.org/10.1016/j.enbuild.2018.01.063.

[33] S. Jerez, I. Tobin, R. Vautard, J. Montávez, J.M. Lopez-Romero, F. Thais, B. Bartok, O. Christensen, A. Colette, M. Déqué, G. Nikulin, S. Kotlarski, E. Meijgaard, C. Teichmann, M. Wild, The impact of climate change on photovoltaic power generation in Europe, Nature Commun. 6 (2015) 10014, http://dx.doi.org/10.1038/ncomms10014.

[34] X. Li, D.L. Mauzerall, M.H. Bergin, Global reduction of solar power generation efficiency due to aerosols and panel soiling, Nat. Sustain. 3 (9) (2020) 720–727, http://dx.doi.org/10.1038/s41893-020-0553-2.

[35] J. Houston, Evaporation in the Atacama Desert: An empirical study of spatio-temporal variations and their causes, J. Hydrol. 330 (3) (2006) 402–412, http://dx.doi.org/10.1016/j.jhydrol.2006.03.036.

[36] CORDEX, Coordinated regional climate dowscaling experiment, 2022, https://cordex.org/. (Accessed 28 January 2022).
[37] R. Moss, M. Babiker, S. Brinkman, E. Calvo, T. Carter, J. Edmonds, I. Elgizouli, S. Emori, L. Erda, K. Hibbard, R. Jones, M. Kainuma, J. Kelleher, J.F. Lamarque, M. Manning, B. Matthews, J. Meehl, L. Meyer, J. Mitchell, N. Nakicenovic, B. O'Neill, R. Pichs, K. Riahi, S. Rose, P. Runci, R. Stouffer, D. van Vuuren, J. Weyant, T. Wilbanks, J.P. van Ypersele, M. Zurek, Towards New Scenarios for Analysis for Emissions, Climate Change, Impacts, and Response Strategies, Intergovernmental Panel on Climate Change, Geneva, 2008, p. 132, http://dx.doi.org/10.5194/gmd-4-543-2011.
[38] CORDEX, Coordinated regional climate dowscaling experiment, 2022, https://esg-dn1.nsc.liu.se/search/cordex/. (Accessed 23 September 2022).
[39] D. Jacob, A. Elizalde, A. Haensler, S. Hagemann, P. Kumar, R. Podzun, D. Rechid, A.R. Remedio, F. Saeed, K. Sieck, C. Teichmann, C. Wilhelm, Assessing the transferability of the regional climate model REMO to Different COordinated Regional climate downscaling experiment (CORDEX) regions, Atmosphere 3 (1) (2012) 181–199, http://dx.doi.org/10.3390/atmos3010181.
[40] W.J. Collins, N. Bellouin, M. Doutriaux-Boucher, N. Gedney, P. Halloran, T. Hinton, J. Hughes, C.D. Jones, M. Joshi, S. Liddicoat, G. Martin, F. O'Connor, J. Rae, C. Senior, S. Sitch, I. Totterdell, A. Wiltshire, S. Woodward, Development and evaluation of an Earth-System model – HadGEM2, Geosci. Model Dev. 4 (4) (2011) 1051–1075, http://dx.doi.org/10.5194/gmd-4-1051-2011.
[41] B. Stevens, M. Giorgetta, M. Esch, T. Mauritsen, T. Crueger, S. Rast, M. Salzmann, H. Schmidt, J. Bader, K. Block, R. Brokopf, I. Fast, S. Kinne, L. Kornblueh, U. Lohmann, R. Pincus, T. Reichler, E. Roeckner, Atmospheric component of the MPI-M Earth System Model: ECHAM6, J. Adv. Modelling Earth Syst. 5 (2) (2013) 146–172, http://dx.doi.org/10.1002/jame.20015.
[42] M. Bentsen, I. Bethke, J.B. Debernard, T. Iversen, A. Kirkevåg, Ø. Seland, H. Drange, C. Roelandt, I.A. Seierstad, C. Hoose, J.E. Kristjánsson, The Norwegian Earth System Model, NorESM1-M – Part 1: Description and basic evaluation of the physical climate, Geosci. Model Dev. 6 (3) (2013) 687–720, http://dx.doi.org/10.5194/gmd-6-687-2013.
[43] D. Jacob, A. Elizalde, A. Haensler, P. Hagemann, R. Podzun, D. Rechid, A. Remedio, F. Saeed, K. Sieck, C. Teichmann, C. Wilhelm, Assessing the transferability of the regional climate model REMO to Different COordinated Regional climate downscaling experiment (CORDEX) regions, Atmosphere (3) (2012) 181–199, http://dx.doi.org/10.3390/atmos3010181.
[44] M. Lagos-Zúñiga, R. Balmaceda-Huarte, P. Regoto, L. Torrez, M. Olmo, A. Lyra, D. Pareja-Quispe, M.L. Bettolli, Extreme indices of temperature and precipitation in South America: trends and intercomparison of regional climate models, Clim. Dynam. (2022) http://dx.doi.org/10.1007/s00382-022-06598-2.
[45] S. Feron, R. Cordero, A. Damiani, P. Llanillo, J. Jorquera, E. Sepulveda, V. Asenciom, D. Laroze, F. Labbe, J. Carrasco, G. Torres, Observations and projections of heat waves in South America, Sci. Rep. 3 (9) (2019) http://dx.doi.org/10.1038/s41598-019-44614-4.
[46] M.S. Reboita, R.P. da Rocha, C.A.d. Souza, T.C. Baldoni, P.L.L.d.S. Silva, G.W.S. Ferreira, Future projections of extreme precipitation climate indices over South America based on CORDEX-CORE multimodel ensemble, Atmosphere 13 (9) (2022) http://dx.doi.org/10.3390/atmos13091463.
[47] H. Hersbach, B. Bell, P. Berrisford, S. Hirahara, A. Horányi, J. Muñoz-Sabater, J. Nicolas, C. Peubey, R. Radu, D. Schepers, A. Simmons, C. Soci, S. Abdalla, X. Abellan, G. Balsamo, P. Bechtold, G. Biavati, J. Bidlot, M. Bonavita, G. De Chiara, P. Dahlgren, D. Dee, M. Diamantakis, R. Dragani, J. Flemming, R. Forbes, M. Fuentes, A. Geer, L. Haimberger, S. Healy, R.J. Hogan, E. Hólm, M. Janisková, S. Keeley, P. Laloyaux, P. Lopez, C. Lupu, G. Radnoti, P. de Rosnay, I. Rozum, F. Vamborg, S. Villaume, J.-N. Thépaut, The ERA5 global reanalysis, Q. J. R. Meteorol. Soc. 146 (730) (2020) 1999–2049, http://dx.doi.org/10.1002/qj.3803, Publisher: John Wiley & Sons, Ltd.
[48] D. Jiao, N. Xu, F. Yang, K. Xu, Evaluation of spatial-temporal variation performance of ERA5 precipitation data in China, Sci. Rep. 11 (1) (2021) 17956, http://dx.doi.org/10.1038/s41598-021-97432-y.
[49] R. Urraca, T. Huld, A. Gracia-Amillo, F.J.M. de Pison, F. Kaspar, A. Sanz-Garcia, Evaluation of global horizontal irradiance estimates from ERA5 and COSMO-REA6 reanalyses using ground and satellite-based data, Sol. Energy 164 (2018) 339–354, http://dx.doi.org/10.1016/j.solener.2018.02.059.
[50] J. Olauson, ERA5: The new champion of wind power modelling? Renew. Energy 126 (2018) 322–331, http://dx.doi.org/10.1016/j.renene.2018.03.056.
[51] M. Tarek, F.P. Brissette, R. Arsenault, Evaluation of the ERA5 reanalysis as a potential reference dataset for hydrological modelling over North America, Hydrol. Earth Syst. Sci. 24 (5) (2020) 2527–2544, http://dx.doi.org/10.5194/hess-24-2527-2020.
[52] D. Tetzner, E. Thomas, C. Allen, A validation of ERA5 reanalysis data in the Southern Antarctic Peninsula—Ellsworth land region, and its implications for ice core studies, Geosciences 9 (7) (2019) http://dx.doi.org/10.3390/geosciences9070289.
[53] M. Belmonte Rivas, A. Stoffelen, Characterizing ERA-interim and ERA5 surface wind biases using ASCAT, Ocean Sci. 15 (3) (2019) 831–852, http://dx.doi.org/10.5194/os-15-831-2019.
[54] J. Mayer, M. Mayer, L. Haimberger, Consistency and homogeneity of atmospheric energy, moisture, and mass budgets in ERA5, J. Clim. 34 (10) (2021) 3955–3974, http://dx.doi.org/10.1175/JCLI-D-20-0676.1.
[55] M. Trolliet, J.P. Walawender, B. Bourlès, A. Boilley, J. Trentmann, P. Blanc, M. Lefèvre, L. Wald, Downwelling surface solar irradiance in the tropical Atlantic Ocean: a comparison of re-analyses and satellite-derived data sets to PIRATA measurements, Ocean Sci. 14 (5) (2018) 1021–1056, http://dx.doi.org/10.5194/os-14-1021-2018.
[56] R.M. Graham, S.R. Hudson, M. Maturilli, Improved performance of ERA5 in Arctic gateway relative to four global atmospheric reanalyses, Geophys. Res. Lett. 46 (11) (2019) 6138–6147, http://dx.doi.org/10.1029/2019GL082781.
[57] E. Radziemska, The effect of temperature on the power drop in crystalline silicon solar cells, Renew. Energy 28 (1) (2003) 1–12, http://dx.doi.org/10.1016/S0960-1481(02)00015-0.
[58] S. Jerez, I. Tobin, R. Vautard, J.P. Montávez, J.M. López-Romero, F. Thais, B. Bartok, O.B. Christensen, A. Colette, M. Déqué, G. Nikulin, S. Kotlarski, E. van Meijgaard, C. Teichmann, M. Wild, The impact of climate change on photovoltaic power generation in Europe, Nature Commun. 6 (1) (2015) 10014, http://dx.doi.org/10.1038/ncomms10014.
[59] R. Chenni, M. Makhlouf, T. Kerbache, A. Bouzid, A detailed modeling method for photovoltaic cells, Energy 32 (9) (2007) 1724–1730, http://dx.doi.org/10.1016/j.energy.2006.12.006.
[60] T.E. Oliphant, Python for scientific computing, Comput. Sci. Eng. 9 (3) (2007) 10–20, http://dx.doi.org/10.1109/MCSE.2007.58.
[61] S. Bayo-Besteiro, A. Perez-Alarcón, Python code, 2022, http://dx.doi.org/10.5281/zenodo.7178476, Zenodo 9/10/2022.
[62] J.A. Añel, The importance of reviewing the code, Commun. ACM 54 (5) (2011) 40–41, http://dx.doi.org/10.1145/1941487.1941502.
[63] D. Carvalho, A. Rocha, M. Gómez-Gesteira, C. Silva Santos, Offshore wind energy resource simulation forced by different reanalyses: Comparison with observed data in the Iberian Peninsula, Appl. Energy 134 (2014) 57–64, http://dx.doi.org/10.1016/j.apenergy.2014.08.018.
[64] J. Moemken, M. Reyers, H. Feldmann, J.G. Pinto, Future changes of wind speed and wind energy potentials in EURO-CORDEX ensemble simulations, J. Geophys. Res.: Atmos. 123 (12) 6373–6389, http://dx.doi.org/10.1029/2018JD028473.
[65] P. Ferrada, F. Araya, A. Marzo, E. Fuentealba, Performance analysis of photovoltaic systems of two different technologies in a coastal desert climate zone of Chile, Sol. Energy 114 (2015) 356–363, http://dx.doi.org/10.1016/j.solener.2015.02.009.
[66] E. Fuentealba, P. Ferrada, F. Araya, A. Marzo, C. Parrado, C. Portillo, Photovoltaic performance and LCoE comparison at the coastal zone of the Atacama Desert, Chile, Energy Convers. Manage. 95 (2015) 181–186, http://dx.doi.org/10.1016/j.enconman.2015.02.036.
[67] R.R. Cordero, A. Damiani, D. Laroze, S. MacDonell, J. Jorquera, E. Sepúlveda, S. Feron, P. Llanillo, F. Labbe, J. Carrasco, J. Ferrer, G. Torres, Effects of soiling on photovoltaic (PV) modules in the Atacama Desert, Sci. Rep. 8 (1) (2018) 13943, http://dx.doi.org/10.1038/s41598-018-32291-8.